The Statistics of Interfibre Contact in Random Fibre Networks

W.W. SAMPSON and J. SIRVIÖ

*Theory is presented describing the fraction of fibre surfaces in a random fibrous network that contact zero, one or two other fibres. A full model gives these absolute contact states in terms of the fractional contact area (*FCA*) and mean coverage of the network. An approximate model gives the absolute contact states as a function of* FCA *only. The expressions derived are compared with experimental data and agreement is excellent.*

Voici une théorie qui décrit la fraction des surfaces des fibres dans un réseau aléatoire de fibres en contact avec aucune, 1 ou 2 autres fibres. Un modèle détaillé donne ces états de contact absolu selon la surface de contact fractionnelle (SCF) et l'étendue moyenne du réseau. Un modèle approximatif fournit les états de contact absolu en tant que fonction de la SCF uniquement. Les expressions dérivées sont comparées aux données expérimentales, et la concordance est excellente.

JPPS

W.W. Sampson
School Materials
Univ. Manchester
PO Box 88
Manchester M60 1QD UK
(sampson@manchester.ac.uk)
J. Sirviö
KCL Sci. Consulting
PO Box 70
FIN-02151 Espoo
Finland

INTRODUCTION

Much of the literature concerning the strength of paper quantifies the extent of interfibre bonding by the relative bonded area (*RBA*) of the fibres in the sheet, this being defined as the expected fraction of fibre surface that is bonded to other fibres. Whereas sheet strength is affected by bonding and not by contact, it is the latter property that can be modelled through probabilistic treatments of network structure. Additionally, although interfibre bonds may occur only where fibres are sufficiently close to each other to be considered to be in contact, it can be diffcult to distinguish between bonds and contacts experimentally [1]. The structural property analogous to *RBA* is the fractional contact area (*FCA*), i.e. the expected fraction of the fibre surface that is in contact with other fibres. *FCA* represents an upper bound on *RBA* such that, when all regions of interfibre contact are bonded, *RBA* and *FCA* are equivalent [2].

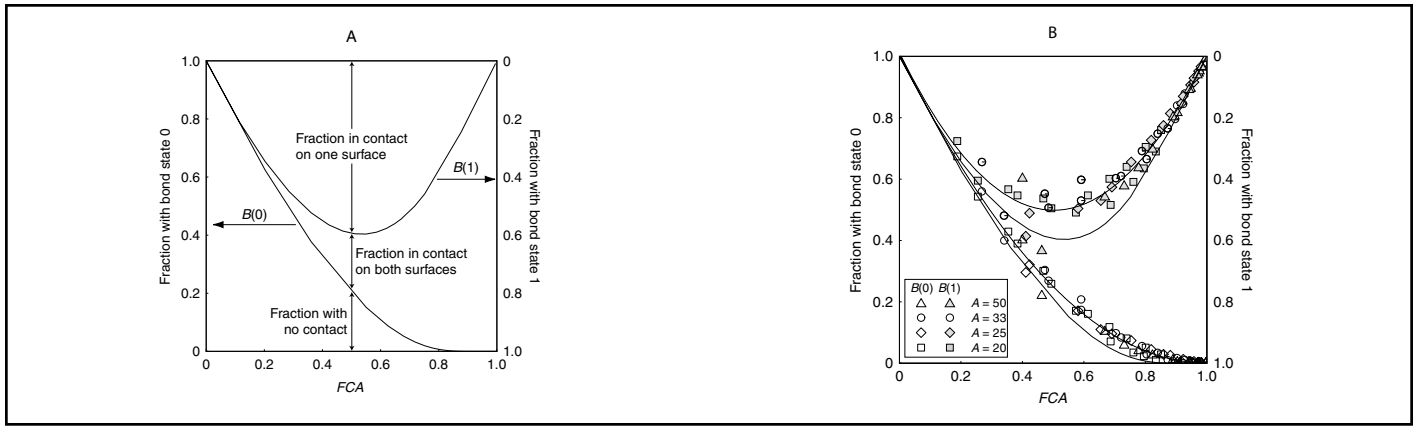

Fig. 1. The contact state diagrams after Kallmes et al. [8]. (A) Contact states given by Eqs. (4–6) for two-dimensional networks. The vertical arrows show the fractions with each contact state at *FCA* = 1/2. (B) Comparison with simulation data for fibres of various aspect ratios, *A*. Broken lines approximate the multiplanar model given in [8].

Models describing fibre contact usually consider random fibre networks, where the fibre centres are distributed according to a point Poisson process in two dimensions and the orientation of the major axes of fibres to a given direction has a uniform distribution. The number of fibres covering a point is a discrete random variable c and, in a network of mean coverage $\bar{c}$, the Poisson probability that a point has coverage c is given by

$$P(c) = \frac{\bar{c}^{c} e^{-\bar{c}}}{c!} \qquad \text{for } c = 0, 1, 2, 3 \ldots \qquad (1)$$

We note from Eq. (1) that the statistics of coverage are independent of fibre geometry and are influenced by the mean coverage only. This means that, for the models that we consider here, we do not need to assume any particular fibre geometry. We bear in mind, however, that the mean coverage of a sheet can be influenced through selection of fibres because the mean coverage of a sheet with mean grammage $\bar{\beta}$ formed from fibres of width ω and coarseness δ is

$$\bar{c} = \frac{\bar{\beta}\omega}{\delta} \qquad (2)$$

Phenomena such as fibre orientation and flocculation result in the in-plane structure of industrially formed sheets being manifestly different from those of random fibre networks formed from the same constituent fibres, and the nature and extent of these differences can be used to provide insights into the forming process [3]. Interestingly, the structure of flocculated networks perpendicular to the plane of the sheet, as manifested in the pore height distribution and the distribution of density in the plane, is not significantly different from that of random fibre networks [4–7].

In very thin networks, say those with mean coverage less than ~1, only a small fraction of the network has coverage greater than 3 and, wherever fibres cross, they can be considered to be in contact. We classify these thin networks as two-dimensional networks and the *FCA* for these, Φ_{2D} was derived by Kallmes et al. [8] by considering the Poisson probabilities of the network having coverage 1, 2 or 3 to give

$$\Phi_{2D} = 1 - \frac{1 - e^{-\bar{c}}}{\bar{c}} \qquad (3)$$

At higher values of mean coverage, we expect that there will be regions where one fibre lies above another but is separated by some vertical distance through the influence of nearby fibres. Expressions for the *FCA* of networks of this type are given as a function of mean network coverage and porosity in [2].

Now, at any given point in the plane of a network, a fibre covering that point may be in contact with one, two or no other fibres above or below it, no other configuration being possible. These absolute contact states are important because we expect regions where there is no contact to exhibit different stress–strain behaviours from those with one or two contacts. Similarly, we might expect the fracture path through a sheet to be influenced to some extent by the configuration of fibre contacts and the compression behaviour of a given fibre segment within a sheet, to be determined by the local number and configuration of contacts and those of nearby regions. Kallmes et al. [8] considered the distribution of absolute contact states in two-dimensional networks and gives the probability of absolute contact states 0, 1 and 2 respectively as

$$B(0) = e^{-\bar{c}} \qquad (4)$$

$$B(1) = \frac{2}{\bar{c}}\left(1 - \left(1 + \bar{c}\right) e^{-\bar{c}}\right) \qquad (5)$$

$$B(2) = \frac{1}{\bar{c}}\left(\bar{c} - 2 + \left(\bar{c} + 2\right) e^{-\bar{c}}\right) \qquad (6)$$

Kallmes et al. presented these expressions in a representation referred to as the bonding state diagram; this is reproduced in Fig. 1A and we term this the contact state diagram instead. The diagram is produced by plotting Eqs. (4) and (5) against the *FCA* as given by Eq. (3). Thus, the only variable used to generate these curves is the mean coverage of the network.

Now, Eqs. (3–6) apply only to networks with mean coverage less than ~1 and, from Eq. (3), this corresponds to an *FCA* of ~0.4. Of course, we know that the *RBA*, and therefore the *FCA,* of sheets with a given grammage is influenced by processes such as refining and wet-pressing. As such, above the very low coverages required for two-dimensional models, sheets with any given coverage may exhibit a range of values of *FCA*; thus, the use of mean coverage as the only variable to calculate absolute contact states should be used with caution.

This comment has been made elsewhere [3,9] and, indeed, Kallmes et al. provided theory for the contact states of fibres in multiplanar networks formed by the superposition of two-dimensional networks with a given probability of contact occurring between pairs of layers obscured by a third. The resulting expressions are rather unwieldy and require numerical evaluation; accordingly, they are omitted here but can be found in the appendix to [8]. We note, however, that these are functions of the number of layers, the coverage of a two-dimensional layer and a free parameter giving the probability of contact between layers. This final parameter is effectively the *FCA* in addition to that for two-dimensional networks, though its relationship with *FCA* was not discussed by Kallmes et al.

Kallmes et al. compared their theory with data generated in a simulation where rectangular fibres of constant length and various aspect ratios, *A*, were placed in a rectangular computational grid. The coordinates of fibre centres and the orientation of the major axes of fibres were generated as uniformly distributed random numbers. These data are included in the contact state diagram shown in Fig. 1B. The broken lines represent second-order polynomial regressions on the data. In the original work, these lines were given by the theory for multiplanar networks; insufficient information is given in [8] to allow these same curves to be generated here, but the curves shown are qualitatively similar.

To date, the work of Kallmes et al. remains the only significant study of the distribution of absolute contact states in planar random fibre networks. While the simulation data in Fig. 1B show reasonable agreement with theory for multiplanar networks, not all of the required variables are well characterized; the theory for two-dimensional networks is more robust, but agreement with the data is poor. Here, we develop theory that allows the absolute contact states of fibres to be calculated directly from comparatively simple expressions in terms of

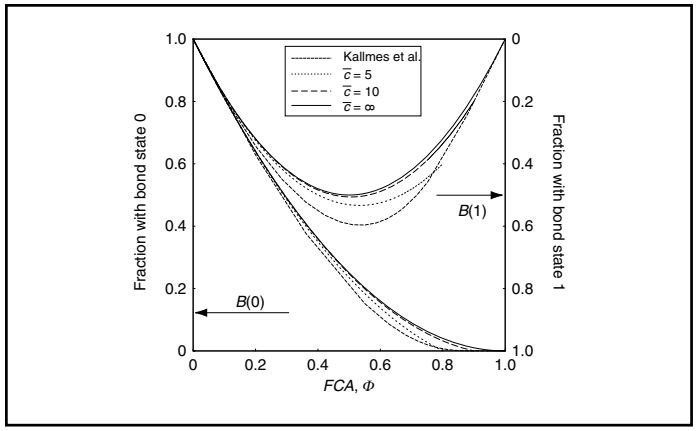

Fig. 2. Contact state diagram showing the dependence of contact states on mean coverage. At a given $\bar{c}$, the maximum value of Φ is ~1–1/$\bar{c}$.

TABLE I
SUMMARY OF FURNISHES AND HANDSHEET PROPERTIES

Identifier	Furnish	Fraction	Grammage (gm^{-2})	Density (kgm^{-3})
TMP	TMP	LFF	65.2	279
UKL	Unrefined kraft	LFF	66.5	499
RKL	Refined kraft	LFF	66.0	647
RKW-40	Refined kraft	WP	43.7	624
RKW-65			65.1	664
RKW-100			108.4	708

The fractions LFF and WP denote the long fibre fraction and whole pulp, respectively.

two variables only: the mean coverage of the network and its *FCA*. The theory presented allows these parameters to be decoupled fully. Also, we present the results of an experimental programme to quantify the absolute contact states of fibres in handsheets and to compare the model with the data arising.

THEORY

First, we consider a random fibre network of infinite coverage, before proceeding to consider networks of finite coverage.

In a network of infinite coverage, the fraction of fibre surfaces contacting other fibres is the *FCA*, Φ, such that a fraction $(1 - \Phi)$ of fibre surfaces is not in contact with other fibres. At any given point in the network, a given fibre may be in contact with one, two or no other fibres above or below it, with the probability of contact on each side of the fibre being Φ. It follows that absolute contact states for networks of infinite coverage are given by

$$B_\infty(0) = (1-\Phi)^2 \tag{7}$$

$$B_\infty(1) = 2\Phi(1-\Phi) \tag{8}$$

$$B_\infty(2) = \Phi^2 \tag{9}$$

where the coefficient 2 in Eq. (8) is included to account for the two possible configurations of one-sided contact, i.e. contact above and below a given fibre.

Finite Coverage

Now, the model of Kallmes et al. for two-dimensional networks assumes that all crossings between fibres generate a contact; the treatment given above for networks of infinite thickness considers fibre contacts independently of the number of fibre crossings at any given point. To derive corresponding expressions for networks of finite coverage, we must consider both the number of crossings at any point and the probability that these generate a contact.

It turns out that, in networks of finite mean coverage $\bar{c}$, the expressions of Kallmes et al. provide some bounds on the absolute contact states of the network:

— $B(0)$ is the fraction of the fibre length in the network that may only have contact state 0 and cannot have contact state 1 or 2.

— $B(1)$ is the fraction of the fibre length in the network that may have contact state 0 or 1 but cannot have contact state 2.

— $B(2)$ is the fraction of the fibre length in the network that can have any of the three permissible contact states.

Now, the *FCA*, Φ, is the fraction of all fibre surfaces that are in contact and, since the outer surfaces of fibres at the top and bottom of the sheet are not available for contact, the probability of contact between fibres, Φ_s, will be somewhat greater than Φ. At any point in the network with coverage c, the number of surfaces is 2 c and, of these, two are not available for contact. Thus, to a reasonable approximation, we expect the probability of contact between fibres Φ_s to be given by

$$\Phi_s \approx \frac{\bar{c}}{\bar{c}-1}\Phi \tag{10}$$

Equation (10) carries with it an important implication: while the probability of contact Φ_s may take values between 0 and 1, the *FCA* Φ may only take values between 0 and $(\bar{c}-1)/\bar{c}$. So we may state that the upper limit on *FCA* and, hence, on *RBA*, is determined by the mean coverage of the network.

We consider contacts at points only, so the cross-sectional geometry of fibres, their flexibility and, hence, their propensity to conform to each other, are not an issue. If we assume that the probability that a given point on a fibre's surface is in contact with another fibre Φ_s is independent of the coverage at that point, then the fractions of the network with contact states 0, 1 and 2 are given by, respectively,

$$B^*(0) = B(0) + (1-\Phi_s)B(1) + (1-\Phi_s)^2 B(2) \tag{11}$$

$$B^*(1) = \Phi_s B(1) + 2\Phi_s(1-\Phi_s)B(2) \tag{12}$$

$$B^*(2) = \Phi_s^2 B(2) \tag{13}$$

such that, as $\bar{c} \to \infty$, Eqs. (11–13) recover Eqs. (7–9) and as $\Phi_s \to 1$, they recover Eqs. (4–6).

Few paper grades are made with mean coverage less than ~5 and, above this value, the term $e^{-\bar{c}}$ in Eqs. (4–6) becomes negligible. Noting this and substituting for Φ_s, $B(0)$, $B(1)$ and $B(2)$ in Eqs. (11–13) yields

$$B^*(0) \approx 1 + \Phi\left(\Phi - 2 - \frac{\Phi}{(\bar{c}-1)^2}\right) \tag{14}$$

$$B^*(1) = 2\Phi\left(1 - \Phi + \frac{\Phi}{(\bar{c}-1)^2}\right) \tag{15}$$

$$B^*(2) \approx \left(1 - \frac{1}{(\bar{c}-1)^2}\right)\Phi^2 \tag{16}$$

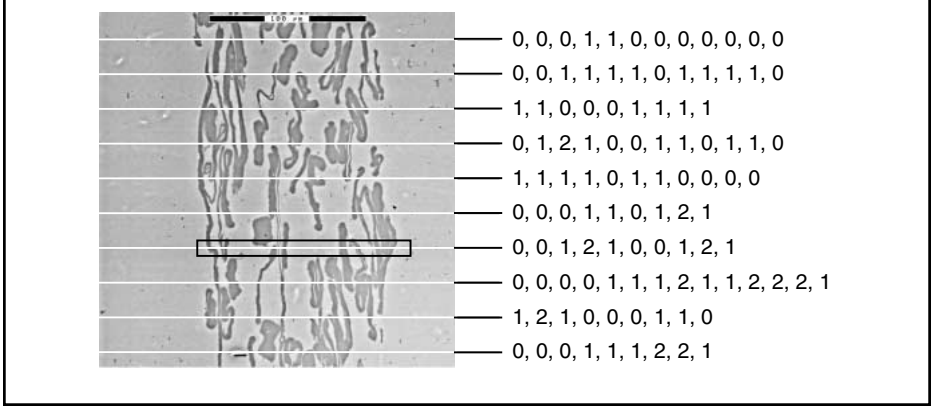

Fig. 3. Example image of a sheet cross-section, with z-directional sampling lines and schema for the characterization of contact states. An enlarged image of the boxed region is shown in Fig. 4.

Equations (14–16) are plotted as a contact state diagram in Fig. 2. The curves of Kallmes et al. are included for comparison and the maximum value of *FCA* used is $(\bar{c}-1)/\bar{c}$, as discussed. The difference between the new theory and the expressions of Kallmes et al. is clear and, as expected, increases with increasing coverage. We observe that, when the mean coverage is greater than 10, the curves are close to those predicted for networks of infinite coverage. It is important to note, however, that the maximum *FCA* approaches 1 at much higher coverages. At maximum contact, the fraction of fibres with contact state 1 is ~$2/\bar{c}$ and that with contact state 2 is ~ $1-2/\bar{c}$.

TABLE II
DATA ARISING FROM ANALYSIS OF SHEET CROSS-SECTIONS

	Number of fibres	Number of contacts	$\bar{c}$	Φ	Contact state *B*(0)	*B*(1)	*B*(2)
TMP	814	146	8.1	0.179	0.674	0.296	0.029
UKL	1110	363	11.1	0.327	0.468	0.418	0.114
RKL	950	422	9.5	0.444	0.301	0.518	0.181
RKW-40	635	218	6.4	0.343	0.431	0.450	0.118
4KW-65	912	373	9.1	0.409	0.338	0.511	0.151
RKW-100	1448	611	14.5	0.422	0.340	0.475	0.184

EXPERIMENTAL

In order that the validity of the theory could be tested, several sets of handsheets were prepared for analysis. The model is influenced only by mean coverage and *FCA*, and these two variables were altered by choice of pulps, refining and grammage. Experimental conditions and sheet properties are summarized in Table I. The TMP had freeness 40 mL and was produced at KCL, Espoo, Finland from fresh spruce chips using the pilot Sunds Defibrator RGP 42 refiner. Pulps UKL and RKL were a commercial bleached kraft pine pulp; UKL was unrefined and RKL was refined with a Voith-Sulzer, single-disk refiner at a specific edge load of 2.5 Wsm^{-1} and a specific refining energy of 150 $kWht^{-1}$. The sheets formed from these three pulps were made with a target grammage of 65 gm^{-2} from the long fibre (+14/+28) fraction from a Bauer-McNett classifier to minimize the influence of fines on consolidation and to aid the identification of contacts. Three further sets of sheets with nominal grammages 40, 65 and 100 gm^{-2} were formed from a laboratory-cooked and bleached kraft pine pulp beaten for 1000 revolutions in a PFI mill. As the beating was so light, sheets were formed from the whole pulp. All handsheets were formed according to ISO 5269-1 [10] and grammage and density determined according to ISO 536 [11] and EN 20534 [12], respectively.

Samples from each handsheet were embedded under vacuum in an epoxy resin (Epon-812, Electron Microscopy Services, Hatfield, UK). After curing, cross-sections were prepared using a Struers DAP-V, Struers A/S, Ballerup, Denmark, mechanical grinding and polishing unit so as to minimize the occurrence of artifacts that might arise though sectioning with a microtome. For each sample, 10 cross-sections were imaged using an ElectroScan 2020, FEI Co., Hillsboro, OR, USA, scanning electron microscope (SEM) in back-scatter mode at a magnification of X400. Ten uniformly spaced sampling lines were drawn over each image in the z direction of the sheet and the number of fibres intersecting each line and the contact state of each of these fibres was recorded.

The process of identifying and counting contacts was one of visual assessment and is illustrated by example via Figs. 3 and 4. Figure 3 shows an SEM image of a cross-section of the unrefined kraft sample; the scale bar represents 100 μm and the row of numbers beside each sampling line corresponds to the contact states of the fibres at the points where they intersect the line. As the processes of embedding and sectioning the samples might damage some points of contact, a qualitative assessment was made where the separation between adjacent fibres was very small and a contact was counted where their contours were considered to be very similar. The classification scheme is illustrated further in Fig. 4, which shows the boxed region of Fig. 3 at higher magnification. Bearing in mind that we count contacts only at the points where fibres intersect the sampling line, we note, for example, that there is void space within Fibres B, E, H and J and that Fibre H contacts the line twice. Note also that Fibre C does not contact the line, but that a small piece of detritus close to it does. Given such complexities in the classification of objects along the scanning lines, we opted to use an experienced

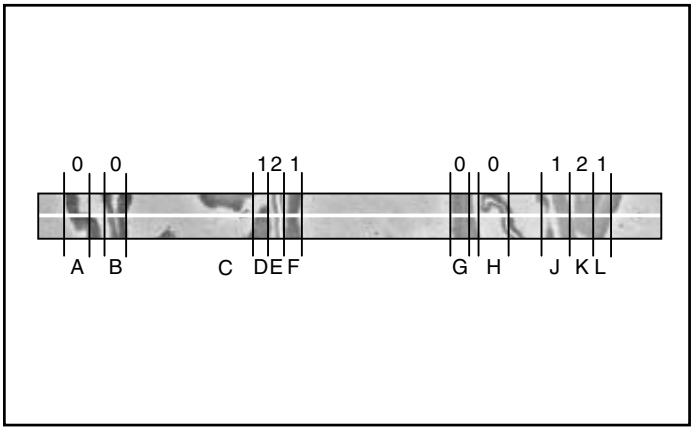

Fig. 4. Enlarged image of the boxed region shown in Fig. 3. Contact states of fibres at their points of contact with the sampling line are shown above each fibre. Note that Fibre C does not contact the sampling line.

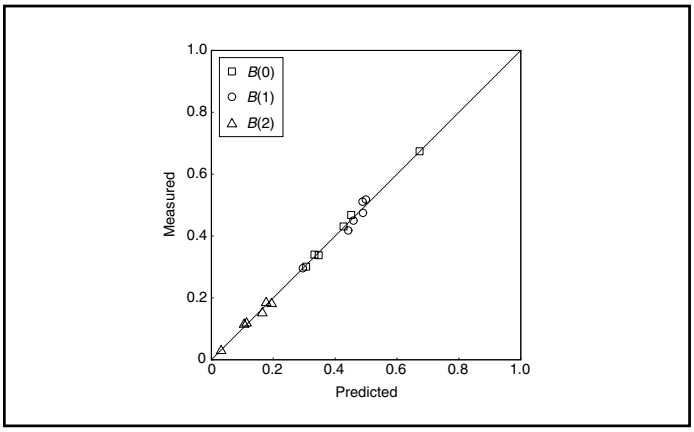

Fig. 5. Comparison of modelled distribution of absolute contact states with experiment. Calculated values were computed using values of coverage and *FCA* from Table II in Eqs. (14–16).

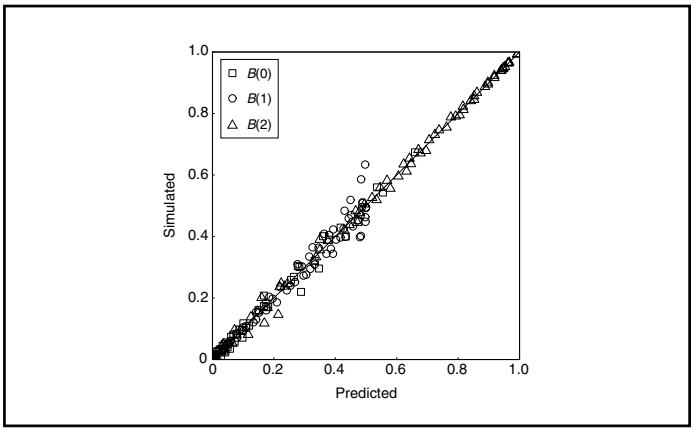

Fig. 6. Comparison of modelled distribution of absolute contact states with simulation data of Kallmes et al. [8]. Calculated values were computed using Eqs. (7–9).

human operator to characterize and count contacts rather than to seek to develop an image-analytic rule-based procedure. Of course, we recognize that there is an element of subjectivity to our technique, though the data that we present in the sequel suggest that the errors in classification were either minimal or acted disproportionately in favour of the predictions of our model.

For the example in Fig. 3, we have recorded the contact states at points of 107 fibres intersecting 10 lines: 46 points have contact state 0, 50 have contact state 1 and 11 have contact state 2. Our estimate of the expected coverage in the image is given by the number of fibres that intersect lines divided by the number of lines, and so is 10.7. The total number of contacts is given by half the number of fibres with contact state 1 plus the number with contact state 2, and so for our example is 36. The *FCA* Φ is given by the number of contacts divided by the number of fibres, and so for our example is 0.336. The process was repeated for 10 images of each sample such that 100 sampling lines were analyzed. The data are collated and summarized in Table II.

Using the values of Φ and $\bar{c}$ given in Table II, we have computed the values of $B(0)$, $B(1)$ and $B(2)$ using Eqs. (14–16). These are compared with the observed values in Fig. 5; linear regression on the data yields a line of unit gradient passing through the origin with coefficient of determination, $r^2 = 0.995$. When using the model for networks of infinite coverage, it seemed appropriate to substitute the probability of contact Φ_s for the fractional contact area Φ in Eqs. (7–9); when doing this, regression on the data yielded a line with gradient 1.01 and coefficient of determination 0.934. However, when the value of Φ was used in the model for infinite coverage, the calculated values of $B(0)$, $B(1)$ and $B(2)$ differed from those plotted in Fig. 5 in the third decimal place only, such that the regression data are almost unaffected. Thus, while the infinite coverage model neglects the unavailability of fibre surfaces at the outer surfaces of the network, this can be compensated for by reducing the probability of contact, such that it is given by the *FCA* Φ. Certainly, this approach is simpler than the full model given by Eqs. (14–16) and it yields the same distribution of contact states to any degree of accuracy achievable in measurements. It is worth noting also that the very high values of the coefficient of determination arise in part because the sum of $B(0)$, $B(1)$ and $B(2)$ must be 1. As such, an underestimate in one or two of the predictions will yield a corresponding overestimate in the third and vice versa. Nonetheless, we note that, for the data presented here, the greatest difference between the measured and modelled contact states was 0.024.

As discussed above, Kallmes et al. [8] provided simulation data for *FCA*, $B(0)$, $B(1)$ and $B(2)$. As coverages were not reported in [8], we have compared these data with the model for networks of infinite coverage as given by Eqs. (14–16). The comparison is shown in Fig. 6 and regression on these data yields a line with unit gradient and a coefficient of determination 0.993.

CONCLUSIONS

Models have been presented that allow calculation of the distribution of absolute contact states of fibres in random networks. An approximate model, where the only variable is the *FCA* between fibres, has been shown to give arguably the same accuracy as a more complete model that includes the mean coverage of the network as a second variable. Agreement between the models and experimental data is excellent, as is that between the models and simulation data from the literature.

REFERENCES

1. PAGE, D.H., TYDEMAN, P.A. and HUNT, M., "A Study of Fibre-to-Fibre Bonding by Direct Observation" in Formation and Structure of Paper, Trans. 2nd Fund. Res. Symp., 1961, F. Bolam, Ed., Pulp Paper Fund. Res. Soc., 171–193, FRC, Manchester (2003).
2. SAMPSON, W.W., "The Statistical Geometry of Fractional Contact Area in Random Fibre Networks", *J. Pulp Paper Sci.* 29(12):412–416 (2004).
3. SAMPSON, W.W., "The Structural Characterisation of Fibre Networks in Papermaking" in The Science of Papermaking, Trans. 12th Fund. Res. Symp., C.F. Baker, Ed., Pulp Paper Fund. Res. Soc., 1205–1288 (2001).
4. DODSON, C.T.J., "On the Distribution of Pore Heights in Random Layered Fibre Networks" in The Science of Papermaking, Trans. 12th Fund. Res. Symp., C.F. Baker, Ed., Pulp Paper Fund. Res. Soc., 1037–1042 (2001).
5. DODSON, C.T.J., OBA, Y. and SAMPSON, W.W., "Bivariate Normal Thickness-Density Structure in Real Near-Planar Stochastic Fibre Networks", *J. Statist. Phys.* 102(1/2):345–353 (2001).
6. NISKANEN, K. and RAJATORA, H., "Statistical Geometry of Paper Cross-Sections", *J. Pulp Paper Sci.* 28(7):228–233 (2002).
7. HOLMSTAD, R., "Methods for Paper Structure Characterisation by Means of Image Analysis", PhD Thesis, NTNU, Trondheim, Norway (2004).
8. KALLMES, O., CORTE, H. and BERNIER, G., "The Structure of Paper, V. The Bonding States of Fibres in Randomly Formed Papers", *Tappi J.* 46(8):493–502 (1963).
9. DENG, M. and DODSON, C.T.J., Paper: An Engineered Stochastic Structure, TAPPI PRESS (1994).
10. "Pulps – Preparation of Laboratory Sheets for Physical Testing – Part I: Conventional Sheet-Former Method", ISO 5269-1, Intl. Org. Standardiz., Geneva, Switzerland (1998).
11. "Paper and Board – Determination of Grammage", ISO 536, Intl. Org. Standardiz., Geneva, Switzerland (1995).
12. "Bestimmung der Dicke und der scheinbaren Stapeldichte oder scheinbaren Blattdichte", EN 20534, Europ. Comm. Standardiz., Brussels, Belgium (1993).

REFERENCE: SAMPSON, W.W. and SIRVIÖ, J., The Statistics of Interfibre Contact in Random Fibre Networks, Journal of Pulp and Paper Science, 31(3):127–131 July/August/September 2005. Paper offered as a contribution to the Journal of Pulp and Paper Science. Not to be reproduced without permission from the Pulp and Paper Technical Association of Canada. Manuscript received February 8, 2005; revised manuscript approved for publication by the Review Panel June 23, 2005.

KEYWORDS: STATISTICS, FIBER NETWORKS, FIBERS, CONTACTING, MATHEMATICAL MODELS.